Visualization of Magnetization Reversal in the Buried Layer of an Exchange-spring Magnet

C. R. Kmety,[1] D. Haskel,[1] J. C. Lang,[1] G. Srajer,[1] J. S. Jiang,[2] S. D. Bader[2]
[1]Advanced Photon Source and [2]Materials Science Division, Argonne National Laboratory, Argonne, IL, U.S.A.

Introduction

The magnetization reversal process is of fundamental interest in magnetism as well as being technologically significant. An exchange-spring magnet consists of hard and soft ferromagnetic layers coupled at the interface. The combination of the high magnetic anisotropy of the hard phase with the high magnetization of the soft phase results in an enhanced maximum energy product. The system of our study has the soft Fe layer on top of the hard SmCo layer.

Previous work [1] reported on the rotation of the remanent magnetization of the soft layer from the initial saturation direction in response to the *conjectured* partial inversion of the magnetization in the adjacent hard layer. Images collected by using a surface-sensitive (magneto-optical indicator film) technique indicate that the Fe magnetization twists and only partially untwists after the application and removal of a large enough negative field. The twist angle increases with the magnitude of the applied negative field. Therefore, an unusual noncollinear (at an angle) coupling of the two ferromagnetic layers in direct contact results. Combining the experimental findings with theoretical considerations, the authors inferred the corresponding behavior of the remanent magnetization in the SmCo layer. The ability to actually “see” the reversal process in the hard layer is crucial for investigating the microscopic origin of the switching.

In this article, we present real-space images of the local remanent magnetization of Sm during the reversal process with micrometer resolution. The evolution of the relative fraction of inverted domains is monitored as a function of the magnetic field applied opposite to the initial saturation. Our capability to probe the magnetic microdomain structure allowed the observation of the nearly zero (average) remanence described by equal areas of opposite magnetizations. All measurements were performed on the same sample and in similar experimental conditions as those described in Ref. 1.

Methods and Materials

X-ray spectromicroscopy measurements were performed at the Synchrotron Radiation Instrumentation Collaborative Access Team (SRI-CAT) 4-ID-D insertion device beamline at the APS. Our technique combines x-ray magnetic circular dichroism (XMCD) with x-ray microfocusing to determine the local magnetic moment. We use right- and left-handed circularly polarized x-rays to irradiate the sample, and we measure the corresponding absorption coefficients through the fluorescence yield from the sample. Photons with opposite helicities are absorbed differently if the sample has nonzero local magnetic moment. The flipping ratio, defined as the normalized difference in the intensities of the right and left circular components, provides the projection of the local magnetization vector along the beam direction. The x-ray focusing optics consist of a pair of mirrors in the Kirkpatrick-Baez (KB) configuration, which focuses the beam to a minimum spot size of about $1.2 \times 2.5\ \mu m^2$. Focused x-rays are incident on the sample at an angle of 45° from the surface, and the magnetic field is applied parallel to the sample surface along the easy axis of the magnetization. Images of magnetic domain configuration in the SmCo layer were obtained at the Sm L_3 edge by scanning the sample through the focused spot.

The sample is a SmCo/Fe bilayer thin film with strong uniaxial anisotropy. The layers were grown epitaxially by magnetron sputtering on a MgO(110) substrate having a nominal structure of MgO/Cr(20 nm)/SmCo(20 nm)/Fe(20 nm)/Cr(5 nm). The easy magnetization axis is along the in-plane c axis of SmCo. The macroscopic easy-axis magnetization loops exhibit separate switching transitions for the Fe and SmCo layers [1].

Results and Discussion

Two series of XMCD images reveal the magnetization reversal process in the ferromagnetic SmCo layer buried underneath the Fe layer [Fig. 1(a) and 1(b)]. Each of these local magnetization maps was acquired in zero field after saturation in one (positive) direction (along the easy axis of the magnetization) and the subsequent application and removal of a magnetic field in the opposite (negative) direction. Individual domains in the SmCo layer are much smaller (~50 nm) than the micrometer beam size; therefore, each pixel represents the average magnetization within spatial resolution through the entire layer thickness. Because of the large uniaxial anisotropy in the hard layer, the magnetization vector of the individual domains is expected to be either parallel or antiparallel to the easy axis. Red and blue colors correspond to areas consisting almost entirely of positive and negative domains, respectively, while the intermediate colors represent mixtures of positive and negative domains in different proportions. Of particular interest is the green

(a)

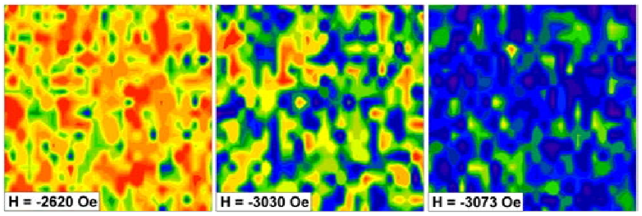

(b)

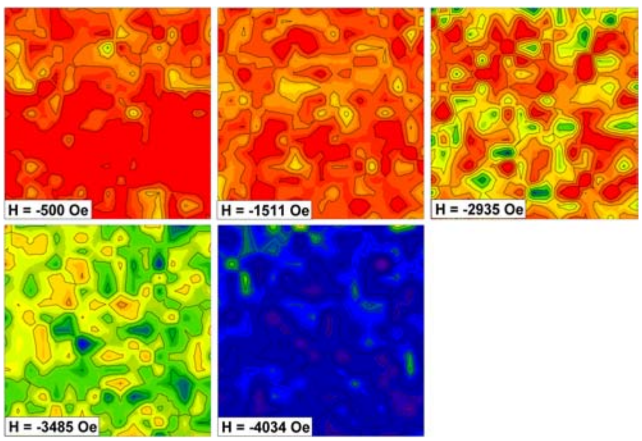

FIG. 1. Sm L_3 edge XMCD images [(a) 125×95 μm^2 and (b) 64×64 μm^2] of the remanent domain structure in the ferromagnetic SmCo layer after applying (and removing) a maximum negative field of (a) -2620 Oe, -3030 Oe, and -3073 Oe, and (b) -500 Oe, -1511 Oe, -2935 Oe, -3485 Oe, and -4034 Oe, to the initially positively saturated magnetization. The color scale ranges from red (positive domains dominate) to green (equal areas of positive and negative domains) to blue (negative domains dominate). The size of the beam used to collect the series of images is (a) 2.7×3.5 μm^2 and (b) 4.8×6.0 μm^2.

(a) *(b)*

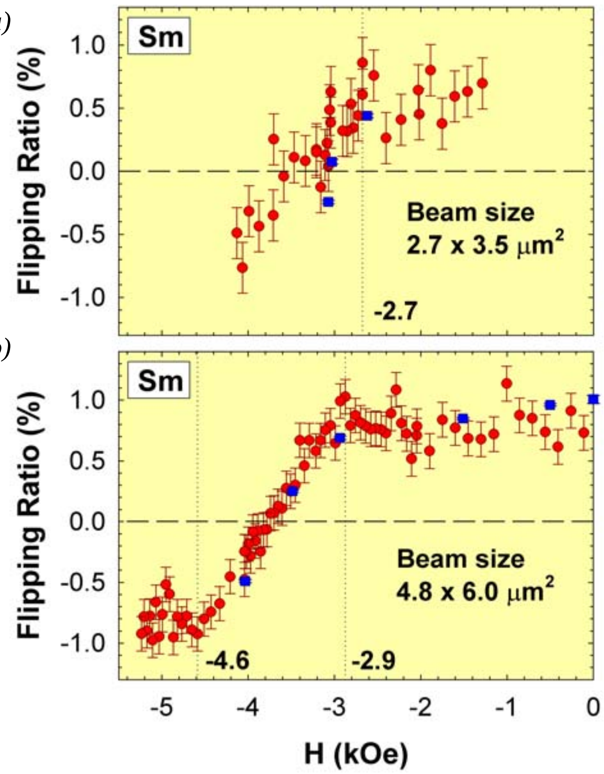

FIG. 2. Local remanent hysteresis (circles) measured by XMCD for the beam-size areas of (a) 2.7×3.5 μm^2 and (b) 4.8×6.0 μm^2 of the SmCo layer. Averaged remanent hysteresis (squares) calculated from the magnetization for the entire area in Fig. 1.

color, which describes the compensated domain state (equal areas of opposite magnetization) characterized by zero remanence. By applying an increasing negative field, the inverted domains progressively increase at the expense of the positive domains, and a contrast reversal occurs. The choice of negative fields was based on the prediction of earlier work [1] that zero remanence can be observed at about -3.1 kOe.

A representative local remanent hysteresis for a beam-size area (Fig. 2(b), circles) demonstrates that at large enough negative fields, the magnetic moments of individual domains start inverting in submicrometer regions, and at saturation, only inverted (negative) domains remain. As the reverse field increases from 0 to -2.9 kOe, the domains enclosed by the beam keep their magnetizations parallel to the initial positive saturation field. The onset of magnetization reversal occurs for a threshold field value of about -2.9 kOe, and the complete inversion from predominantly positive to negative domains is characterized by a switch width of about -1.7 kOe. For negative fields larger than -4.6 kOe, all domains have their magnetizations anti-parallel to the initial positive saturation field. Remanent hysteresis curves recorded at several areas in one image and with slightly different beam sizes show variations in the threshold field value (between 100 to 300 Oe) and switch width (between 1.0 and 1.7 kOe). While the threshold field value might be determined by the spatial variation of local crystallographic domains, the switch width is proportional to the beam size. The images of Fig. 1 allow the extraction of the remanent hysteresis curve averaged over the total area (Fig. 2, squares). Since the averaged and local remanent hystereses are characterized by the same contrast change, all domains in an image participate in the magnetization reversal. Moreover, the contrast change reaches maximum value, indicating the lack of domains with magnetizations away from the easy axis.

Acknowledgments

The authors gratefully acknowledge P. J. Eng for assistance with the KB mirrors and E. Trakhtenberg, D. Shu, and M. M. Lehmuller for participating in the continuous development of the experimental setup. Use of the APS was supported by the U.S. Department of Energy, Office of Science, Office of Basic Energy Sciences, under Contract No. W-31-109-ENG-38.

Reference

[1] V. K. Vlasko-Vlasov, U. Welp, J. S. Jiang, D. J. Miller, G. W. Crabtree, and S. D. Bader, Phys. Rev. Lett. **86**, 4386 (2001).